doi.org/10.36721/PJPS.2025.38.5.REG.13765.1

Synthesis of functionalized benzofuran esters through Suzuki-Miyaura cross-coupling reactions, their DFT and pharmacological studies

Lal Khan and Muhammad Zubair*
Department of Chemistry, Government College University Faisalabad

Abstract: The Suzuki-Miyaura cross-coupling reaction was used to synthesize phenylbenzofuran-2-carboxylate derivatives (4a- 4f). The structural features of the target molecules were analyzed using two computational tools, e.g., molecular docking and DFT studies. Based on computational studies, target molecules were further screened for hemolytic and enzyme inhibitory activity, e.g., anti-urease and α-glucosidase, investigated to evaluate their biological potential. Hemolytic assay findings indicate that synthesized molecules 4a-4f are non-toxic to RBCs, while Compound (4d) and (4a) showed excellent anti-urease and *α*-glucosidase inhibitory activity (IC_{50} =13.38 ±1.75μM and (IC_{50} = 60.5 ±1.53 μM). comparable to standard drugs. DFT and molecular docking predictions of structural features supported the experimental results. Most and least reactive molecules in this series (4a-4f) are identified by comparing energies (ΔE). 4f exhibits the lowest ΔE of 3.20 eV, indicating its least stability in the synthesized series (4a-4f). In contrast, 4b displays the highest ΔE gap of 6.42 eV, suggesting its highest stability and least reactivity. In this work, computational and in vitro methodologies provided complimentary insights for effective molecular screening of drug candidates, specifically in terms of binding affinity and toxicity profiles.

Keywords: Suzuki-Miyaura reaction, benzofuran, Molecular Docking, Anti-urease, α-glucosidase, DFT studies

Submitted on 26-11-2024 – Revised on 03-02-2025– Accepted on 06-03-2025

INTRODUCTION

A systemic metabolic disease that can impact multiple organ systems, including the gastrointestinal tract, is *diabetes mellitus* (Zhou, Zhang *et al*., 2013). Due to its etiological connection to gastric and duodenal diseases, *Helicobacter pylori* is considered a major gastroduodenal pathogen (Rauf, Ahmed *et al*., 2011b). The blood urea level and the length and severity of diabetes were highly correlated (Anwar, Faisal *et al*., 2024) α-glucosidase is found in small intestine's (Khan, Ahmad *et al*., 2021) epithelium (Little, Falace *et al*., 2013), where it breaks down disaccharides and starch into glucose so that the bloodstream can absorb it (Mahat, Singh *et al*., 2019). The rate at which oligosaccharides hydrolytically cleave into monosaccharides is delayed when the intestinal α-glucosidase enzyme is inhibited (Sonia, Chelleng *et al*.). Multimorbidity like *diabetes mellitus* and *H. pylori* infections forced researchers to search drugs with multiple targets (Bener, Ağan *et al*., 2020). In this regard, heterocycles, either natural or synthetic, come as a first choice due to their wide range of applications (Kabir and Uzzaman, 2022). Heterocycles like benzofuran compounds are naturally abundant (Miao, Hu *et al*., 2019) and acts as a fundamental structural unit for the wide variety of naturally existing molecules by exhibiting multidirectional functionalities (Quasdorf, Antoft-Finch *et al*., 2011). Many researchers reported benzo furans derivatives as anti-tumor, anti-viral (Farhat, Alzyoud *et al*., 2022), (Xu, Yang *et al*., 2017), anti-bacterial (Promchai, Janhom *et al*., 2020) and anti-oxidative agents (Bharani, Rao *et al*., 2025, Kwiecień and Wodnicka, 2020). Some of the FDA-approved drugs have been shown in (fig. 1a) (Dwarakanath and Gaonkar, 2022). Spasov *et al.,* reported the synthesis of the most potent acyl benzofurans (a) as α-glucosidase inhibitors with hypoglycemic potential (Spasov, Babkov *et al*., 2017). Similarly, Boukharsa *et al*. described the most potent Benzofuran-Pyridazines (b) as α-glucosidase inhibitors (Boukharsa, Karrouchi *et al*., 2023). Taha and coauthors reported benzofuran-based-thiazoldinones (c) as the most potent inhibitors (Taha, Rahim *et al*., 2020). Azimi *et al*. also developed the most potent biphenyl pyrazole-benzofurans (d) as urease inhibitors (Azimi, Azizian *et al*., 2021a) (fig. 1b). For the synthesis of substituted benzofurans (Mundhe, Bhanwala *et al*., 2023), iso-benzofuran and spiro-benzofuran (Nair, Basu *et al*., 2023) many reactions are employed, among these, the Suzuki-Miyaura reaction is a frequently used for desired cross-coupling reaction (Beletskaya, Alonso *et al*., 2019) in organic and medicinal chemistry (Bhattacherjee, Rahman *et al*., 2021). Suzuki cross-coupling reactions are mostly employed in the organic field(de Robichon, Bordessa *et al*., 2019) to synthesize biologically active molecules (Sharma, Naveen *et al*., 2013) such as benzofurans. (Tollefson, Hanna *et al*., 2015).

MATERIALS AND METHODS

Computational methods

The energy of optimized geometry of synthesized molecules (4a - 4f) was calculated using Gaussian software DFT parameters of B3LYP/6-31G model (Deghady, Hussein *et al*., 2021). Becke's three-parameter exchange function, or B3LYP for short, is widely used in quantum chemical

**Corresponding author:* e-mail: Zubairmkn@gcuf.edu.pk

calculations due to its consistent performance in combination with the nonlocal Lee-Yang-Parr correlation function (Hertwig and Koch, 1997)·(Raghavachari, 2000). The initial molecular geometry of the studied molecule was established using experimental single crystal X-ray analysis. The same calculations (B3LYP method with 6-31G basis set) were used to obtain the optimized structural parameters (El-Shamy, Alkaoud *et al*., 2022). Gaussian 16 was the program used for all of the calculations (Frisch, Trucks *et al*., 2016). Gauss View 6 as graphical interface to visualize the optimized geometry, HOMO-LUMO and Molecular electrostatic potential (MEP) (Dennington, Millam *et al*., 2016).

Molecular docking

For docking studies ligand and receptor protein structures were processed using Avogadro version 1.2.0 and BioVIA Discovery Studio Visualizer v21.1. (DSV) Using Force Field Merck Molecular parameters, the geometry of each synthesized ligand was optimized. For docking, the grid surface was adjusted to cover the entire receptor with its center, ADT version 1.5.7 ADT (AutoDock Tools) software package was used for this purpose. Default docking parameters were set for all ligands docking with receptors. A genetic search algorithm was utilized to calculate binding affinity of the ligand and receptor. The conformation with the lowest energy was selected as the most stable for post-docking study. Using the formula, Ki (inhibition constant) was then calculated:

$\Delta G=RT\ln Ki$

Where, $Ki= e (\Delta G/RT)$, where ΔG is binding affinity in Kcal/mol, R = 1.987 cal/mol/K and T = 298.15 K.

Python Molecular Viewer 1.5.7 and DSV were used to analyze ADT results. Ligand-receptor binding with different atoms and with functional substitution were also checked. A docking score with low kinase inhibition (KI μM) and a more stable conformation of the ligand with the receptor was used for docking analysis.

Hemolytic activity of compounds

The hemolytic assays of the synthesized derivatives was studied via the reported protocol (Shahzadi, Zaib *et al*., 2019)·(Rubab, Abbasi *et al*., 2017). Three milliliters of recently drawn, heparinized bovine blood taken from Clinical Medicine and Surgery department in University of Agriculture's Faisalabad, Pakistan. After centrifuging the blood at 1000xg for 5 min, disposed the plasma and the cells were three times cleaned using five milliliters of sterile, isotonic PBS (pH 7.4) chilled to four degrees Celsius. Maintained 10^8 cells per milliliter of erythrocytes for every test. Each compound was mixed with 100μL of human cells/mL in isolation. Samples incubated at 37°C for 35 minutes after which centrifuged for ten minutes then paced in ice for 5min and again centrifuged for five minutes at 1000xg speed. 100μL of the supernatant were extracted from each tube and ten times diluted with cold (4°C) PBS. Use PBS (phosphate buffer saline) as the negative control and 0.1% v/v Triton X-100 as the positive control, both of which underwent the same procedure. Using μQuant (Bioteck, USA), measured absorbance at 576 nm. For every sample, the percentage of RBC lysis was determined.

Enzymatic activity of compounds (4a-4f)

Urease Inhibition

Urease inhibitory potential of (4a-4f) derivatives was evaluated using reported protocol (Rauf, Ahmed *et al*., 2011a)·(Taha, Ismail *et al*., 2022), in which the reaction mixture consisting of 25 μL jack bean urease (enzymatic solution) and 55 μL phosphate buffer along with 100 mM urea was incubated with 5 μL test derivatives (0.5 mM concentration) for 15 min at 30°C in 96-well plates. By utilizing Weatherburn's (1967) indophenol method to measure the amount of ammonia produced, urease activity was ascertained. (Weatherburn, 1967). In summary, the alkali reagent contained 0.5% w/v NaOH (70 μL) and active chloride NaOCl (0.1%) and the phenol reagent contained 1% w/v phenol (45 μL) and 0.05% w/v sodium nitroprusside) were taken in each well with a final volume of 200 μL. Using a microplate reader (Spectra Max, Molecular Devices, USA), the increase in absorbance was measured at 630 nm after 50 min. Using SoftMax Pro software (Molecular Devices, USA), the results (per minute change in absorbance) were processed. The entire test was conducted in triplicate at pH 6.8. The standard control was thiourea (Ullah, Khan *et al*., 2024). Inhibition percentage calculated using the formula:

$100 - (OD_{testwell}/OD_{control}) \times 100$

α-Glucosidase inhibition

Target molecules (4a-4f) in-vitro α-glucosidase inhibitory potential were performed in 96 microwell plates using the previously described methodology (Ahmed, Rauf *et al*., 2018) with a slight modification each well was filled with 100 μL (100 mM) pH-6 phosphate buffer and then 50 μL of a commercial solution of Saccharomyces cerevisiae α-glucosidase 1U/mL. Each compound dissolved in DMSO (10 μL) added separately in desired well and incubated microplate at 37°C for 10 min. Then 40 μL (5 mM) p-nitrophenyl-α-D-glucopyranoside (p-NPG) solution in each well, the reaction mixture was incubated again at 37°C for 10 minutes. 100 μL of a 0.5 M Tris solution was used to quench the reaction with a Molecular Devices USA Spectra Max spectrometer calibrated to measure p-nitrophenol release at 405 nm. The activity of the synthesized derivatives was evaluated to acarbose as a reference(Ahmed, Rauf *et al*., 2018). Performed every experiment three times, inhibitor-free reaction mixtures were used as negative controls. For the initial screening, a concentration of 200 μM *α*-glucosidase inhibition was used. The IC_{50} value was then determined using the appropriate concentrations and the screened compounds that showed a high percentage of inhibition.

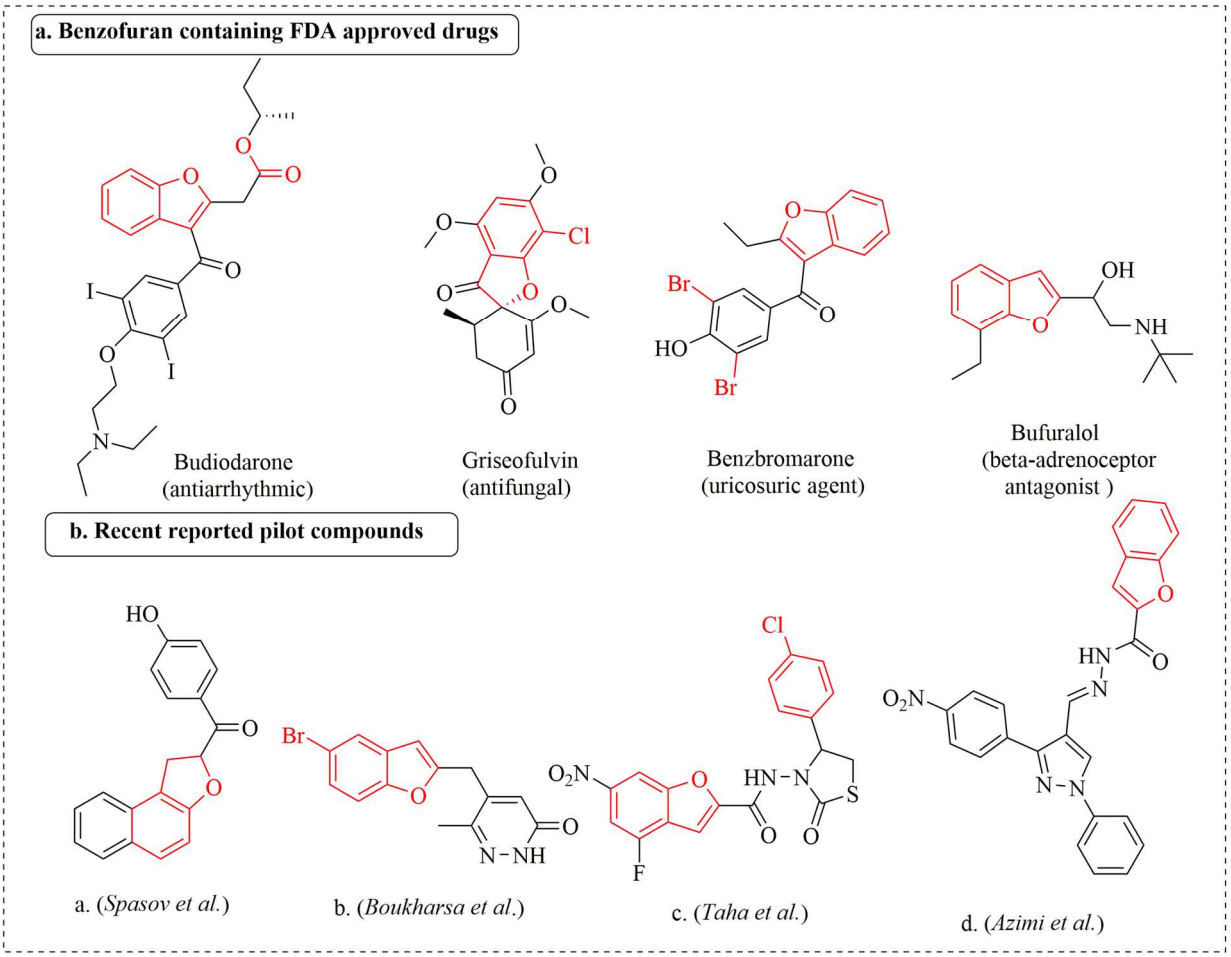

Fig. 1: Summary of benzofuran containing FDA-approved drugs and some recently reported pilot *α*-glucosidase and urease inhibitors.

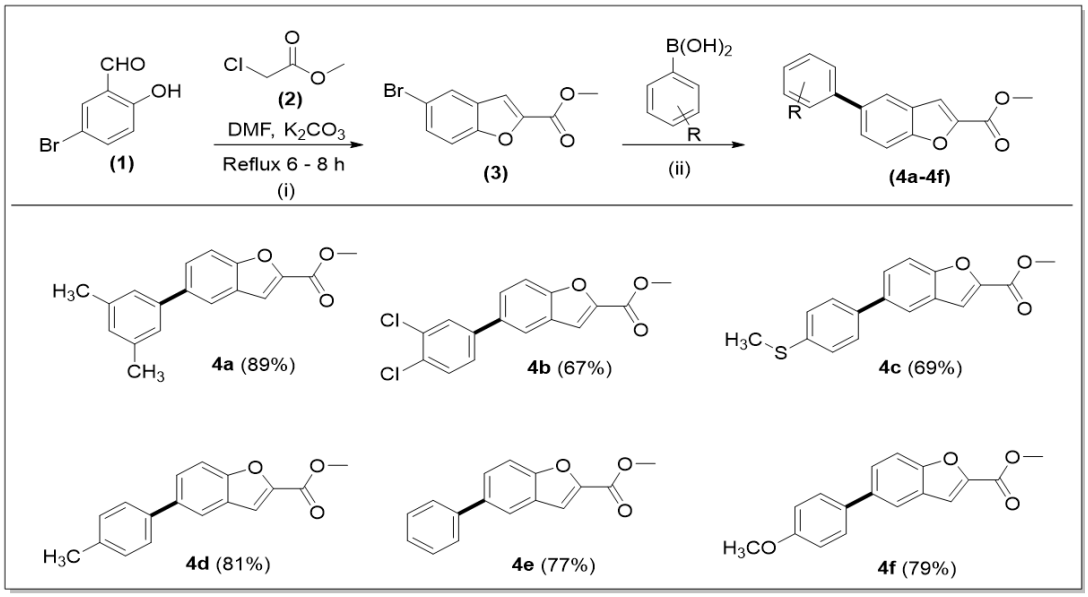

Conditions: (i) Bromosalisalaldehyde (2 g, 0.016mol), DMF (30 ml), methyl chloroacetate (1.91 g, 0.0176 mol), K_2CO_3 (2.43 g, 0.0176 mol),85 °C. (ii) 4a–4f, 1,4-dioxane/water (1:4), Pd (PPh_3)$_4$ (5 mol%), 3 (0.15 g, 0.46 mmol), aryl boronic acid (1.1 eq), K_3PO_4 (2 eq), 16 h reflux at 90 °C.

Scheme 1: Synthesis of Phenyl benzofuran -2-carboxylate derivatives (4a-4f) via Suzuki cross coupling reactions.

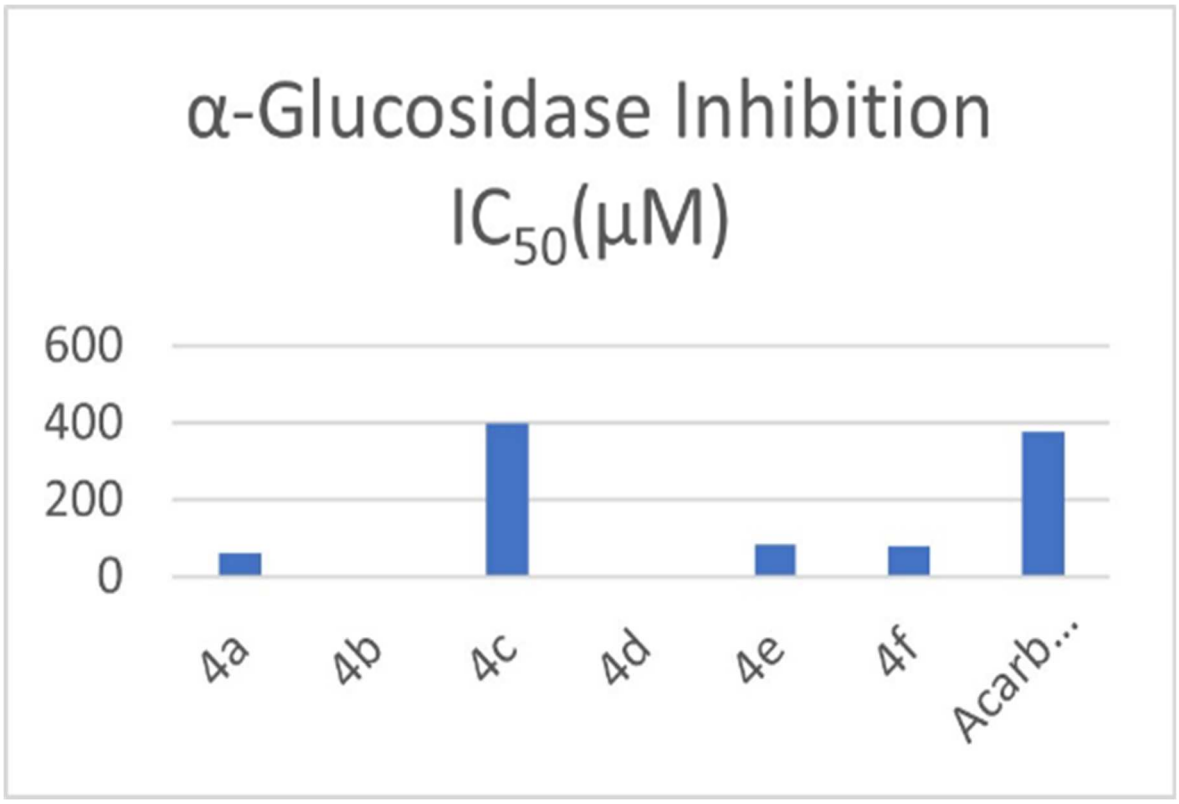

Fig. 2: α-Glucosidase inhibition data of compounds (4a–4f)

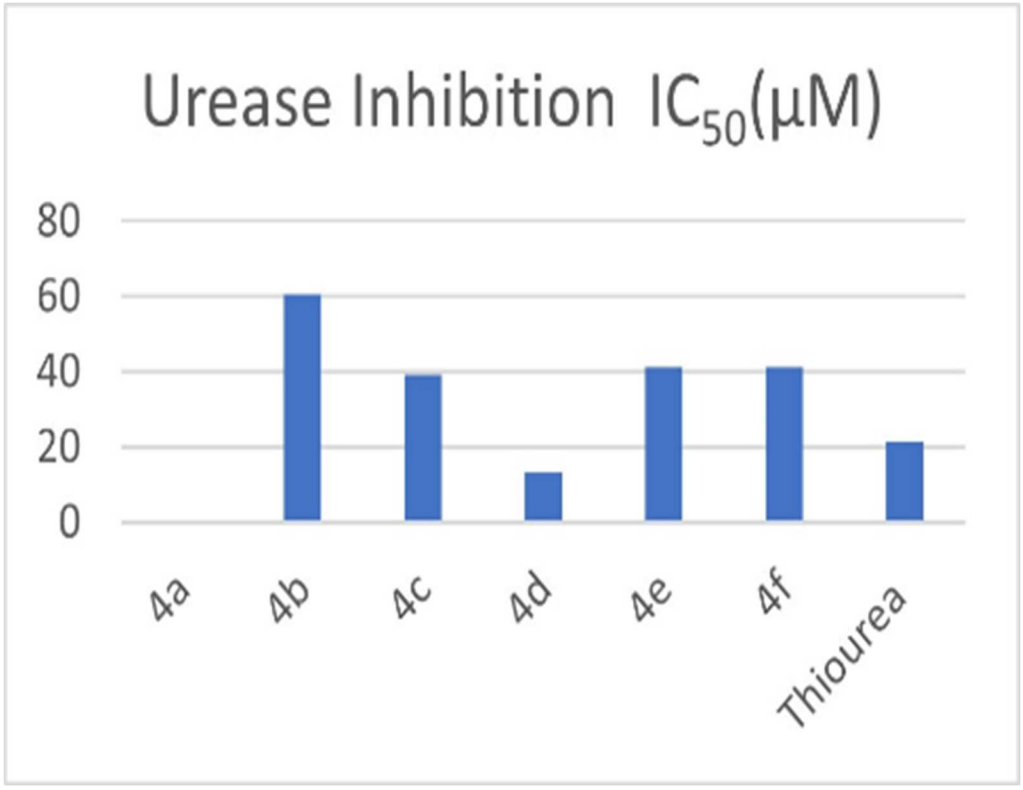

Fig. 3: Anti-urease inhibition data of compounds (4a–4f)

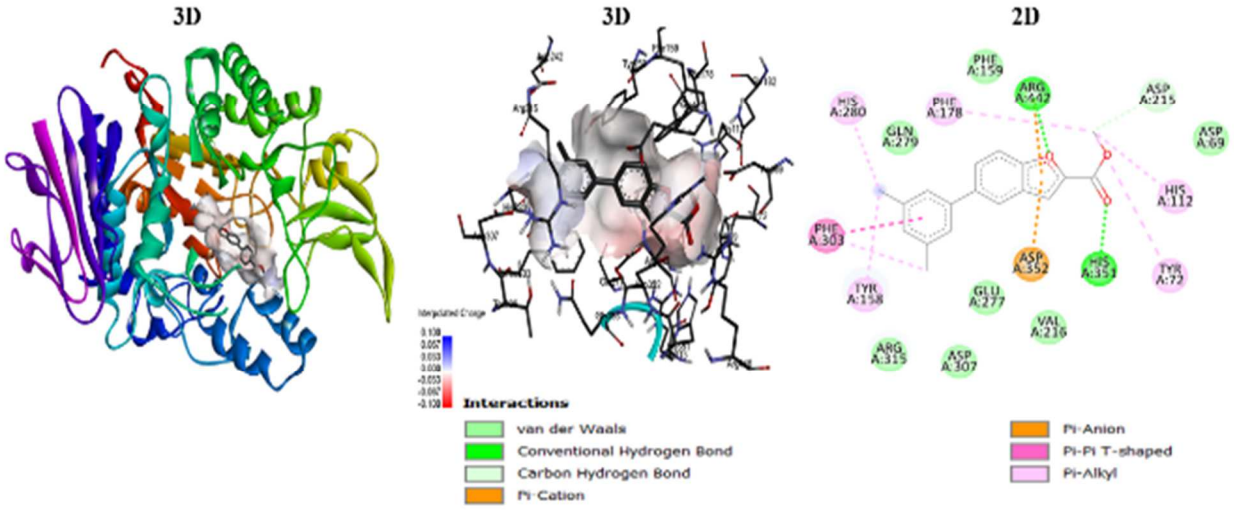

Fig. 4: Molecular docking interactions of 4a

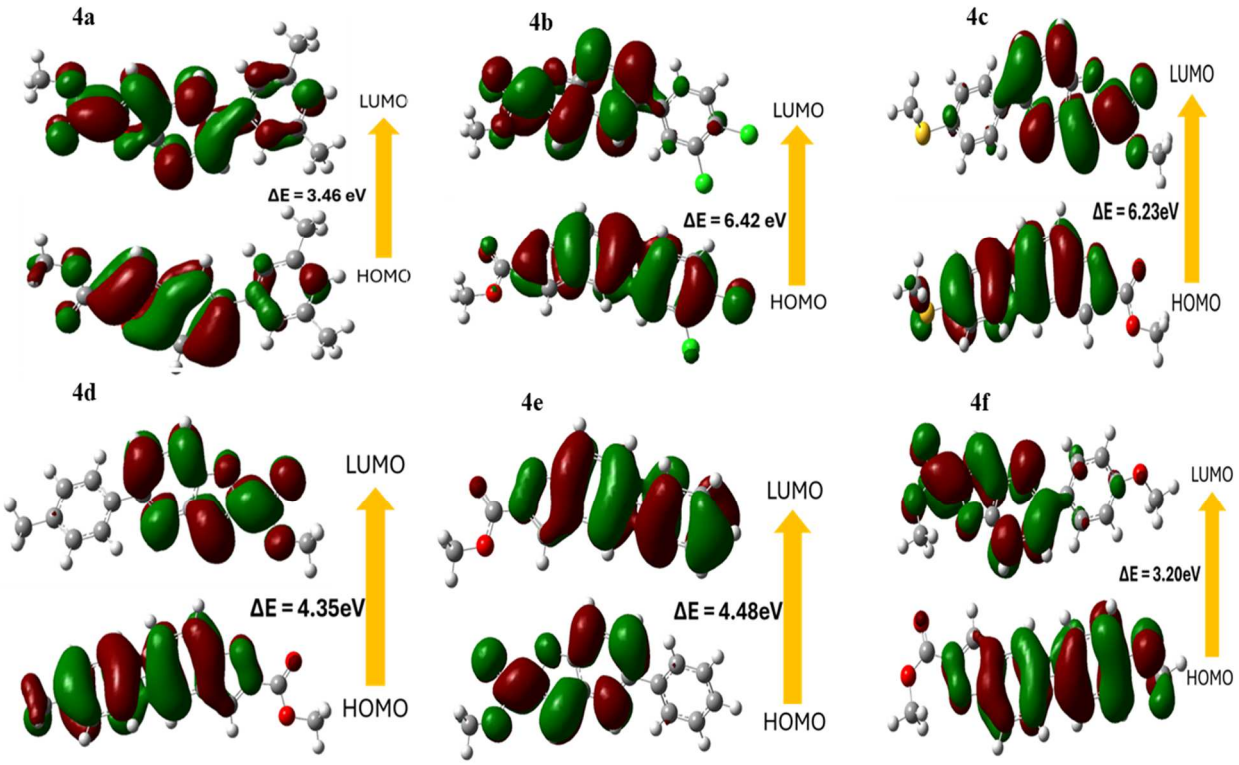

Fig. 5: Molecular Orbitals (HOMO-LUMO) of phenyl benzofuran-2-carboxylate derivatives (4a-4f)

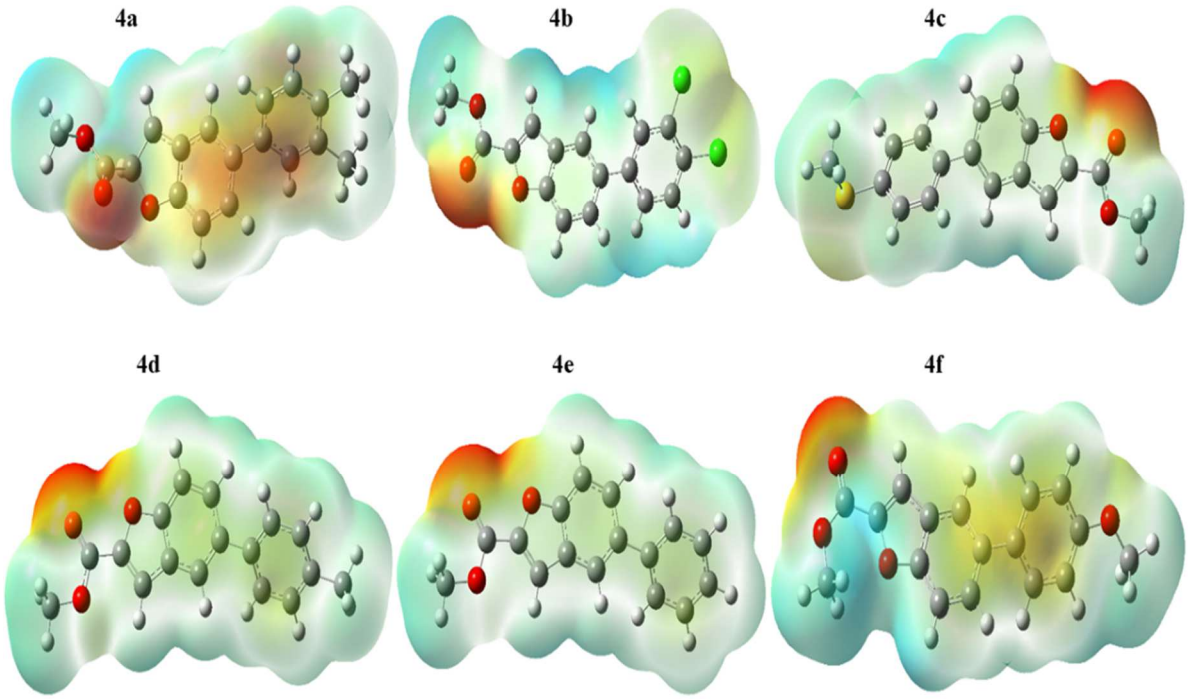

Fig. 6 Electrostatic Potential Surface on molecules (4a-4f).

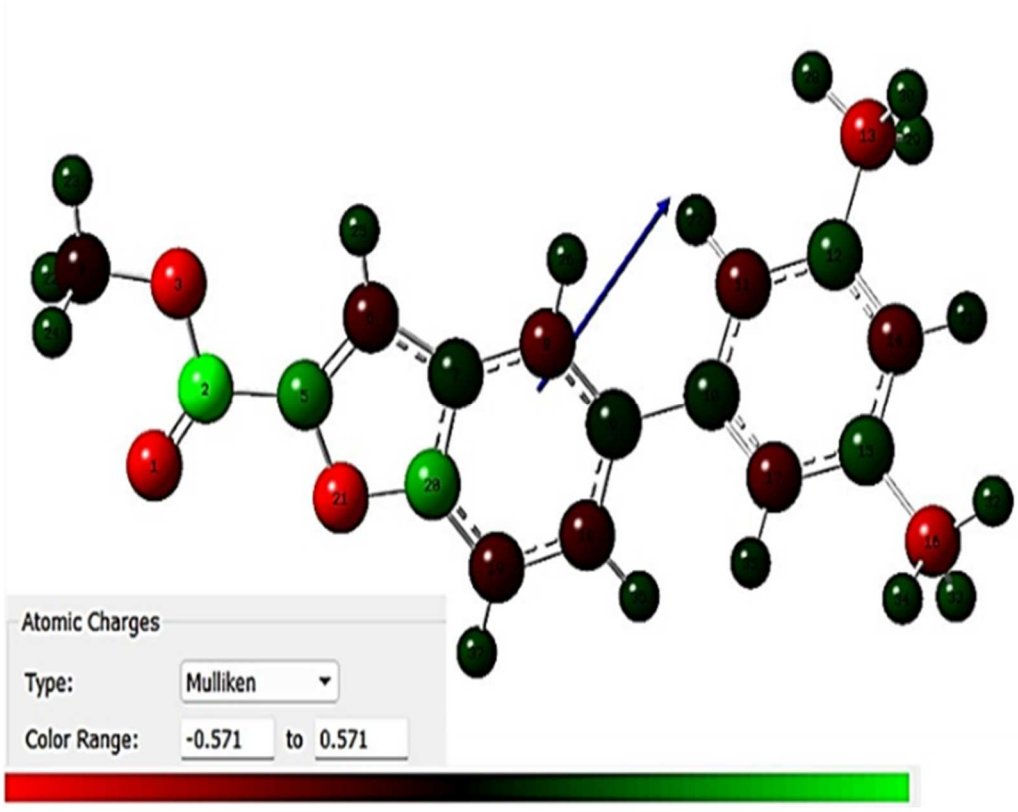

Fig. 7: Mulliken Charges, dipole moment direction on molecule (4a).

General experimental protocol for synthesis of methyl 6-bromo-1H-indene-2-carboxylate

Benzofuran-based ester was synthesized by reacting Bromo salicylaldehyde (2g, 0.016 mmol) with methyl chloroacetate (1.191g, 0.0176 mmol) in the presence of DMF solvent and K_2CO_3 (2.43g,0.0176 mmol) as a base. The reaction mixture was refluxed for six to eight hours (sand bath)**.** Upon completion of the reaction final product was isolated by adding ice-cold distilled water and purified through column chromatography.

General experimental protocol for synthesis of compounds (4a-4f).

Ester of (0.15g, 0.46mmol) **3** and Pd of (0.035g, 5 mol %) was added in a Schlenk flask and 5-6mL solvent of 1, 4-dioxane was added to the mixture for 30-45 min stirring in an inert atmosphere. Then 1.1 eq of aryl boronic acid and 2 eq of K_3PO_4 (2 eq) were added to the distilled water. Refluxed the reaction mixture for a further 12 - 16 h (Scheme 1). Reaction accomplishment was monitored through TLC. After, the product was isolated through column chromatography using n-hexane/ethyl acetate (9:1) and finally became a solid product after evaporating solvent on the rotary evaporator (Hafeez, Sabir *et al*., 2024, Noreen, Bilal *et al*., 2024).

SPECTRAL ANALYSIS

Methyl 5-(3, 5-dimethyl phenyl) benzofuran-2-carboxylate (4a)

Starting with 3 (0.598 m mol, 0.15 g), Pd $(PPh_3)_4$ (2.99 m mol, 0.035 g), K_3PO_4 (0.126 mmol, 0.13 g) and 3, 5-$Me_2C_6H_3B$ $(OH)_2$, (0.68mmol, 0.102 g).Yield 89%, Colorless solid, mp : 124 -125°C. ^{1}H NMR (400 MHz, $CDCl_3$, δ ppm, J Hz): 2.38 (3H, s, CH_3), 3.98 (3H, s, OCH_3), 7 (1H, s, ArH), 7.55 (1H, s, ArH), 7.59 (2H, s, ArH), 7.62 (1H, s, ArH), 7.64 (1H, d,J=4, ArH), 7.82 (1H, d, J=4, ArH); ^{13}C NMR (100 MHz, $CDCl_3$): 52.40 (CH_3), 112.64 (CH), 114.04 (CH), 121.01 (C), 127.23 (CH), 127.50 (CH), 128.63 (CH), 128.99 (CH), 133.43 (C), 136.34 (C), 139.31 (C), 146.11 (C), 155.31 (C), 159.82 (C)

Methyl 5-(3,4-dichlorophenyl)benzofuran-2-carboxylate (4b)

Starting with 3 (0.598 mmol, 0.15 g), Pd$(PPh_3)_4$ (2.99 mmol, 0.035 g), K_3PO_4 (0.126 mmol, 0.13 g) and 3,4-$Cl_2C_6H_3B(OH)_2$, (0.68mmol, 0.129 g). Yield 67%, Colorless solid, mp: 150 -151°C ^{1}H NMR (400 MHz, $CDCl_3$, δ ppm, J Hz): 3.96 (3H, s, OCH_3), 7.8 (1H, s, ArH), 7.4 (1H, d, J=8, ArH), 7.5 (1H, d, ArH), 7.55 (1H, d, ArH), 7.59 (1H, d, j=8 ArH), 7.66 (1H, d, J=8, ArH); ^{13}C NMR (100 MHz, $CDCl_3$): 52.53 (CH_3), 112.82 (CH), 113.98 (CH), 121.14 (C), 126.60 (CH), 127.08 (CH), 127.57 (CH), 129.19 (CH), 130.75 (CH), 131.51 (C), 132.91 (C), 135.12 (C), 140.86 (C), 146.15 (C), 155.43 (C), 159.81 (C)

Methyl 5-(4-(methylthio)phenyl)benzofuran-2-carboxylate (4c)

Starting with 3 (0.598 mmol, 0.15 g), Pd$(PPh_3)_4$ (2.99 mmol, 0.035 g), K_3PO_4 (0.13g, 0.126 mmol) and 4-$MeSC_6H_4B(OH)_2$, (0.68mmol, 0.114 g).Yield 69%, light yellow solid, mp148-149°C : ^{1}H NMR (400 MHz, $CDCl_3$, δ ppm, J Hz): 3.97 (3H, s, OCH_3), 7.81 (1H, s, ArH), 7.3 (1H, d, J=8, ArH), 7.54 (1H, s, ArH), 7.51 (2H, d, J=8, ArH), 7.62 (2H, m, j=12, ArH) ; ^{13}C NMR (100 MHz, $CDCl_3$): 15.83 (CH_3), 52.45 (CH_3) 112.54 (CH), 114.13 (CH), 120.73 (C), 126.93 (CH), 127.22 (CH), 127.46 (CH), 127.77 (CH), 136.91 (C), 137.62 (C), 137.68 (C), 145.96 (C), 155.19 (C),159.90 (C)

Methyl 5-(p-tolyl) benzofuran-2-carboxylate (4d)

Starting with 3 (0.598 mmol, 0.15 g), Pd $(PPh_3)_4$ (2.99 mmol, 0.035 g), K_3PO_4 (0.126 mmol, 0.13 g) and 4-MeC_6H_4B $(OH)_2$, (0.68mmol, 0.0924 g).Yield 81%. Colorless solid, mp 64 °C: ^{1}H NMR (400 MHz, $CDCl_3$, δ ppm, J Hz): 2.24 (3H, s, CH_3), 3.98 (3H, s, OCH_3), 7.8 (1H, s, ArH), 7.6 (1H, d, J=12, ArH), 7.5 (1H, d, J=4, ArH), 7.53 (1H, d, J=4, ArH), 7.44 (1H, d, J=8, ArH), 7.39 (2H, d,J=12, ArH), 7.26 (1H, d, J=4 ArH); ^{13}C NMR (100 MHz, $CDCl_3$): 52.41 (CH_3), 112.47 (CH), 114.15 (CH), 121.08 (C), 125.35 (CH), 127.26 (CH), 127.41 (CH), 127.50 (CH), 128.00 (CH), 137.60 (C), 140.87 (C), 145.96 (C), 155.26 (C), 159.99 (C)

Methyl 5-phenylbenzofuran-2-carboxylate (4e)

Starting with 3 (0.598 mmol, 0.15 g), Pd$(PPh_3)_4$ (2.99 mmol, 0.035 g), K_3PO_4 (0.126 mmol, 0.13 g) and $C_6H_5B(OH)_2$, (0.68mmol, 0.0829 g).Yield 77%, Colorless solid, mp : 98-99 °C. ^{1}H NMR (400 MHz, $CDCl_3$, δ ppm, J Hz): 3.98 (3H, s, OCH_3), 7.84 (1H, s, ArH), 7.44 (2H, t, J=8, ArH), 7.67 (2H, d, J=8, ArH), 7.35 (1H, d, J=8, ArH), 7.61 (1H, d, J=4, ArH), 7.57 (1H, d, J=8, ArH), 7.64 (1H, s, ArH); ^{13}C NMR (100 MHz, $CDCl_3$): 20.48 (CH_3), 52.52 (CH_3), 113.84 (CH), 122.98 (CH), 125.34 (CH),125.79 (C), 127.43 (CH), 129.90 (CH), 130.01 (CH), 130.33 (CH), 130.66 (CH), 135.46 (C), 137.93 (C), 141.36 (C), 145.81 (C), 154.80 (C), 159.92 (C).

Methyl 5-(4-methoxyphenyl) benzofuran-2-carboxylate (4f)

Starting with 3 (0.598 mmol, 0.15 g), Pd $(PPh_3)_4$ (2.99 mmol, 0.035 g), K_3PO_4 (0.126 mmol, 0.13 g) and $C_6H_5B(OH)_2$, (0.68mmol, 0.0829 g). Yield 79%, Colorless solid, mp152 °C**.** ^{1}H NMR (400 MHz, $CDCl_3$) δ 7.52 (1H, d, J= ArH), 7.61(2H, m, ArH),6.98(1H, d, J = 8.6, ArH), 7.79(1H, s, ArH), 7.54 (1H, s, CH), 3.98 (3H, s, OCH_3), 3.85 (3H, s, OCH_3). ^{13}C NMR (100 MHz, CDCl3) δ 159.93(CO), 159.13(C), 154.98(C), 145.86(C), 137.24(C), 133.42(C), 128.40(CH), 126.87(CH), 126.50(CH), 126.46 (CH), 120.32 (CH), 120.22 (CH), 114.28 (CH), 112.39 (CH), 55.35 (OCH_3), 52.42 (OCH_3).

RESULTS

Chemistry

The technique previously described was used to esterify 5-Bromo salicylaldehyde (1) in the present study. Methyl 6-

bromo-1H-indene-2-carboxylate (3) was produced with a 71% yield by reacting compound (1) with methyl chloroacetate (2) (Scheme 1). By refluxing the reaction mixture for six to eight hours, K_2CO_3 served as the catalyst in the aforementioned procedure using Dimethyl Formamide (DMF) as a solvent. By treating (3) through various aryl boronic acids utilizing Pd $(PPh_3)_4$ (catalyst) for the Suzuki coupling at 90 °C, the derivatives of Compound 3 (4a-4f) were effectively created. Here, we carried out similar couplings using a 6:1 water to 1,4-dioxane solvent ratio, yielding newly synthesized benzofuran molecules (4a-4f) in yields ranging from 67 to 89% (Scheme 1, table 1). The increased yield may be due to aryl boronic acid's maximal solvability in 1,4-dioxane/water. Notable are also the highest and lowest yields of thiophene analogues determined by electron-donating and electron-withdrawing processes. The compound (4a) was found to have the highest yield (89%) when the electron-donating group was present. Because of an electron-withdrawing substitution among the benzofuran analogues, (4b) demonstrated a minimum yield of 67% (Scheme 1).

Pharmacological aspects of synthesized compounds (4a-4f)

α-Glucosidase Inhibitory potential

All the synthesized derivatives (4a-4f) were examined for α-Glucosidase Inhibitory potential by using EC3.2.1.20, *Saccharomyces cerevisiae* (α-Glucosidase). The synthesized compounds (4a-4f) demonstrated significant inhibition (47.3 ± 2.30 µM to 78.3 ± 2.44 µM) for α-glucosidase, in comparison to acarbose, (IC_{50} = 375.82 ± 1.76 µM). Among the synthesized compounds, it was observed that the molecule 4a (IC_{50} = 60.5±1.53 µM), which contains two Me groups, demonstrated the highest potency as an inhibitor. It was noteworthy that, the compound (4a) is almost six–times more potent than standard acarbose. It was observed that electron withdrawing groups, led to bit reduction of inhibitory activity. Therefore, compound 4f (IC_{50} = 78.3 ± 2.44 µM) showed a decrease in inhibitory activity owing to methoxy group attached (Azimi, Azizian *et al*., 2021b). The structure-activity relationship has been conducted, primarily influenced by the type, number, position and electron donating or withdrawing nature of substituents (fig. 2).

Urease inhibition study

The synthesized six benzofuran-based derivatives (4a-4f) were characterized using spectroscopic techniques (^{1}H-NMR, ^{13}C-NMR) and subsequently screened for their urease inhibitory potential against enzymes. The molecules in question (4c, 4d, 4e and 4f) exhibited notable inhibitory efficacy, (IC_{50} = 13.38 ± 1.75 µM to 41.35 ± 2.43 µM), in comparison to reference thiourea, (IC_{50} = 21.25 ± 0.15 µM). The synthesized compound (4d) exhibited the highest inhibitory value with (IC_{50} = 13.38 ± 1.75 µM), featuring methyl substitution linked to the benzofuran moiety, demonstrating nearly double the activity compared to thiourea (IC_{50} = 21.25 ± 0.15 µM).

Although (4b) (IC_{50} = 60.49 ± 1.53 µM) exhibited a lower inhibitory effect related to thiourea (IC_{50} = 21.25 ± 0.15 µM), this can be attributed to the presence of two chloro groups, which are characterized by their electron-withdrawing properties. The comparison of the activities of (4b) and (4d) elucidates the effect of substituent evident in the characterization of inhibitory activities. The compounds (4c, 4e and 4f) exhibited activities of (IC_{50} = 39.18 ±1.84 µM, 41.35 ± 2.43 µM and 41.17 ± 1.39 µM) respectively, related to the standard drug thiourea (table 1) (fig. 3).

DISCUSSION

Hemolytic activities of synthesized molecules (4a-4f)

The benzofuran-based analogues (4a-4f) were additionally assessed for their hemolytic properties. The percentage of hemolysis was evaluated and the results are presented in fig. 4. The analysis revealed that molecule (4f) exhibited the lowest toxicity at 11.6%, demonstrating minimal interaction with the RBCs cell membrane in contrast to the standard ABTS, which resulted in a hemolysis rate of 95.9%. It was observed that the most toxic compound identified was derivative (4c), which demonstrated a hemolysis rate of 49.1%. In contrast, the other derivatives 4a (27.7%), 4b (29%), 4d (25%) and 4e (21.6%) showed varying degrees of moderate to low hemolytic activity. SAR was examined in relation to the substituents on the phenyl ring of substituted benzofuran derivatives (4a-4f) to gather a thorough understanding of the hemolytic activities of the synthesized molecules. An analysis of the structures and activities of the compounds under consideration indicates that the inclusion of substituents exhibiting an electron-donating effect tends to result in lower toxicity, in contrast to compounds that possess electron-withdrawing groups, which are generally associated with increased toxicity. Compound 4d (24%), which features methyl substitution on the phenyl ring, exhibits lower toxicity. In contrast, compound 4b (31%) demonstrates increased toxicity, attributable to electron-withdrawing substituent on phenyl ring when compared to the unsubstituted phenyl ring 4e (26%). The activity exhibited a modest decline in dimethyl-substituted derivatives, exemplified by compound (4a), which demonstrated a slight increase in toxicity at 27.3%. The findings indicate that the placement of the functional groups considerably influence the hemolytic potential of the synthesized derivatives (table 1).

Molecular docking

The docking score of synthesized compounds (4a - 4f) against different targets predicted them as excellent enzyme inhibitors most of the compounds show KI value below 3 µM except Compound (4a), which show strong affinity through hydrogen bonding and electrostatic forces

Table 1: α-Glucosidase, Urease inhibition and % Hemolytic activity data of compounds (4a–4f)

Compd.	Urease Inhibition IC_{50}(μM)	α-Glucosidase Inhibition IC_{50}(μM)	% age Hemolytic activity
4a	-----	60.5 ± 1.53	27%
4b	60.49 ± 1.53	---	31%
4c	39.18 ± 1.84	397.5 ± 1.12	49%
4d	13.38 ± 1.75	----	24%
4e	41.35 ± 2.43	81.2 ± 1.33	26%
4f	41.17 ± 1.39	78.3 ± 2.44	11%
Thiourea	21.37 ± 1.76	-	
Acarbose	-	375.82±1.76	
ABTS			95.5%

Table 2: DFT calculations data using B3LYP basis set 6-31G(d, p)

Compound	HOMO (eV)	LUMO (eV)	ΔE (eV)	Energy (Hartree)	Dipole moment (Deby)	*Pearson's absolute hardness* η(eV)	*Mulliken electronegativity* χ(eV)	*electrophilicity indices,* ω *(eV)*
4a	-9.172	-5.707	3.46	-921.27	3.04	1.7325	7.4395	15.97292
4b	-8.480	-2.062	6.42	-1755.55	2.62	3.209	5.271	4.328987
4c	-8.329	-2.097	6.23	-1274.29	2.26	3.116	5.213	4.360618
4d	-6.227	-1.872	4.35	-882.18	4.02	2.1775	4.0495	3.765431
4e	-6.381	-1.897	4.48	-842.86	3.55	2.242	4.139	3.820544
4f	-8.413	-5.212	3.20	-975.13	5.97	1.6005	6.8125	14.49864

with the active site of the ligand residues of chain 50 to 400 i. e. PHE159, GLY160, GLY161, LYS156, TYR158, PHE178. Based on docking results synthesized compounds were subjected to *in vitro* enzymatic studies against the predicted target i.e. *urease* and *α-Glucosidase* Inhibition (fig. 4).

Structural features of synthesized compounds

HOMO and LUMO Analysis

Frontier orbitals, referred to as the HOMO (highest occupied molecular orbital) and LUMO (lowest unoccupied molecular orbital), as significant indicators of electrical properties in quantum chemistry. The transition from HOMO to LUMO orbitals is indicative of light absorption. HOMO orbitals serve as electron donors, whereas LUMO orbitals function as electron acceptors. The surfaces of the frontier orbitals for the compound in question are illustrated in fig. 3. The electron clouds present on the oxygen atoms and the benzofuran ring indicate their involvement in the charge transfer property. Positive and negative signs of the molecular orbital wave function was denoted by red/green, respectively. Since rich electron clouds of π atomic orbitals exist, the electronic transition from HOMO to LUMO is mainly obtained from the electronic π-π* transitions within the molecules (fig. 5). All compounds exhibit a HOMO-LUMO energy gap that indicates their potential as biologically active compounds.

Mulliken Charge Analysis shows electronic charges within the atoms of the molecules and represents the electrophilic and nucleophilic centre within the molecule (fig. 7). The figure shows the Mulliken charge values of the atoms that make up the molecule under study high electron density to positive charge density represented with Red → brown →black→ green → light green colour on a respective atom. Positive charge permeates every hydrogen atom. The most positively charged atom in the molecule is the carbonyl carbon or carbon atom next to the oxygen atom in the furan ring, which represents them as electrophilic centers. At the same time, the electron density mostly resides on oxygen atoms due to their electronegative character. Overall, the electronic cloud resides on aromatic rings. The distribution of electrostatic potential based on molecular electrostatic potential (MEP) makes it a crucial tool for identifying both nucleophilic and electrophilic attacks. Negative electrostatic regions are more favorable to electrophilic attack, while positive electrostatic regions are associated with nucleophilic attack. A color-coded representation of the electrostatic potential ranges in MEP is provided. In target molecules bluish green and red color denote the positive and negative electrostatic region, respectively, while the color yellow denotes the low electron density region. Red → yellow → green → light blue → blue (Deghady, Hussein *et al*., 2021) is the direction in which the positive electrostatic potential on the molecule surface increases (fig. 6,7).

Electrophilicity and hardness

Domingo *et al*. developed single electrophilicity scale was created in 2002 as a result of a thorough study of the

electrophilicity of common reagents used in experimental DA (Diels-Alder) reactions (Domingo, Aurell *et al*., 2002). This scale differentiated organic molecules into strong electrophiles (with $\omega \geq 1.5$ eV), moderate electrophiles (with $0.8 \leq \omega < 1.5$ eV) and marginal electrophiles (with $\omega < 0.8$ eV) categories, while super electrophiles existed for species where $\omega \geq 4.0$ eV. Mainly, strong electrophiles are effective in experiments. The hardness of the molecule indicates how resistant it is to the deformation of the electron cloud during chemical reactions. While soft systems are larger and more polarizable, hard systems are more compact and less polarizable. According to DFT calculations, target molecules fall in soft molecules category (table 2).

CONCLUSION

In the present study, target molecules synthesized from moderate to excellent yield 55 % to 80% using the Suzuki-Miyaura reaction. Their structures were confirmed through NMR analysis which also confirms the successful synthesis. Further structural features of target compounds were evaluated through DFT studies and molecular docking. Considerable interaction between the target compounds and the proteins was confirmed by in-depth structural and computational insights. On the basis of computational predictors, these molecules in vitro studies were performed i.e. *α*-glucosidase, anti-urease, hemolytic and antibacterial. These studies revealed that compounds (4c, 4d, 4e and 4f) and (4a, 4e and 4f) were identified as potential urease and α-glucosidase inhibitors, respectively. Our study's findings suggest that these compounds especially 4a and 4d may be investigated further as potential new medication candidates because of their strong inhibitory action against both anti-diabetic and anti-urease activity.

ACKNOWLEDGMENT

The present data are part of the PhD thesis research work of Lal Khan. The authors gratefully acknowledge the PCSIR (Ministry of Science and Technology), through the data repository of the scientific instrumentation development program initiated in 2021.

Conflict of interest

There is no conflict of interest.

REFERENCES

Ahmed F, Rauf A, Sharif A, Ahmed E, Arshad M, Esposito BP, Kaneko TM and Qureshi AM (2018). A Facile Single Pot Synthesis of Highly Functionalized Tricyclic Heterocycle Compounds via sequential Knoevenagel-Michael addition and their α-glucosidase inhibition, antioxidants and antibacterial Studies. *J. Chem. Soc. Pak.,* **40**(4): 12.

Anwar A, Faisal F, Elahi W, Illahi A, Alam SM, Adnan STA, Batool SA, Bhagwandas S and Hashmi AA (2024). Correlation of blood urea and creatinine levels with thiamin levels in type 1 and type 2 diabetic patients. *Cureus* **16**(3): e57022.

Azimi F, Azizian H, Najafi M, Khodarahmi G, Saghaei L, Hassanzadeh M, Ghasemi JB, Faramarzi MA, Larijani B and Hassanzadeh F (2021a). Design, synthesis, biological evaluation and molecular modeling studies of pyrazole-benzofuran hybrids as new α-glucosidase inhibitor. *Sci. Rep.,* **11**(1): 20776.

Azimi F, Azizian H, Najafi M, Saghaei L, Ghasemi JB, Sadeghi-aliabadi H, Faramarzi MA, Larijani B, Hassanzadeh F and Mahdavi M (2021b). Design and synthesis of novel pyrazole-benzofuran hybrids: *In vitro* α-glucosidase inhibitory activity, kinetic and molecular modeling study. *Res. Square*, (Preprint)

Beletskaya IP, Alonso F and Tyurin V (2019). The Suzuki-Miyaura reaction after the nobel prize. *Coord. Chem. Rev.,* **385**: 137-173.

Bener A, Ağan AF, Al-Hamaq A, Barisik CC, Öztürk M and Ömer A (2020). Prevalence of *Helicobacter pylori* infection among type 2 diabetes mellitus. *Adv. Biomed. Res.,* **9**: 27.

Bharani S, Rao BA, Chowhan LR, Pallepogu R and Prasad MS (2025). Asymmetric synthesis of spiro [benzofuran-pyrrolidine]-indolinedione via bifunctional urea catalyzed [3+ 2]-annulation. *Org. Biomol. Chem. OBC.,* **23**(4): 914-919.

Bhattacherjee D, Rahman M, Ghosh S, Bagdi AK, Zyryanov GV, Chupakhin ON, Das P and Hajra A (2021). Advances in Transition-Metal Catalyzed Carbonylative Suzuki-Miyaura coupling reaction: An update. *Adv. Synth. Catal*., **363**(6): 1597-1624.

Boukharsa Y, Karrouchi K, Anouar EH, Albalwi H, Jarbi I, Ramli Y, Faouzi MEA. Ansar Mh (2023). Synthesis, α-glucosidase and β-galactosidase inhibitory potentials and molecular docking of some novel benzofuran-pyridazine derivatives. *PAC*, **43**(9): 8482-8493.

De Robichon M, Bordessa A, Lubin-Germain N and Ferry A (2019). "CO" as a carbon bridge to build complex C2-branched glycosides using a palladium-catalyzed carbonylative Suzuki-Miyaura reaction from 2-Iodoglycals. *J. Org. Chem.,* **84**(6): 3328-3339.

Deghady AM, Hussein RK, Alhamzani AG and Mera A (2021). Density functional theory and molecular docking investigations of the chemical and antibacterial activities for 1-(4-Hydroxyphenyl)-3-phenylprop-2-en-1-one. *Molecules*, **26**(12): 3631.

Dennington K, Millam T and Semichem J (2016). Gauss View, Version 6 Inc. *Shawnee Mission KS.*

Domingo LR, Aurell MJ, Pérez P and Contreras R (2002). Quantitative characterization of the global electrophilicity power of common diene/dienophile pairs in Diels–Alder reactions. *Tetrahedron*, **58**(22): 4417-4423.

Dwarakanath D and Gaonkar SL (2022). Advances in synthetic strategies and medicinal importance of benzofurans: A review. *Asian J. Org. Chem.,* **11**(8): e202200282.

El-Shamy NT, Alkaoud AM, Hussein RK, Ibrahim MA, Alhamzani AG and Abou-Krisha MM (2022). DFT, ADMET and molecular docking investigations for the antimicrobial activity of 6,6′-Diamino-1,1′,3,3′-tetramethyl-5,5′-(4-chlorobenzylidene)bis[pyrimidine-2,4(1H,3H)-dione]. *Molecules*, **27**(3): 620.

Farhat J, Alzyoud L, Alwahsh M and Al-Omari B (2022). Structure–activity relationship of benzofuran derivatives with potential anticancer activity. *Cancers*, **14**(9): 2196.

Frisch MJ, Trucks GW, Schlegel HB, Scuseria GE, Robb MA, Cheeseman JR, Scalmani G, Barone V, Petersson GA, Nakatsuji H, Li X, Caricato M, Marenich AV, Bloino J, Janesko BG, Gomperts R, Mennucci B, Hratchian HP, Ortiz JV, Izmaylov AF, Sonnenberg JL, Williams, Ding F, Lipparini F, Egidi F, Goings J, Peng B, Petrone A, Henderson T, Ranasinghe D, Zakrzewski VG, Gao J, Rega N, Zheng G, Liang W, Hada M, Ehara M, Toyota K, Fukuda R, Hasegawa J, Ishida M, Nakajima T, Honda Y, Kitao O, Nakai H, Vreven T, Throssell K, Montgomery Jr. JA, Peralta JE, Ogliaro F, Bearpark MJ, Heyd JJ, Brothers EN, Kudin KN, Staroverov VN, Keith TA, Kobayashi R, Normand J, Raghavachari K, Rendell AP, Burant JC, Iyengar SS, Tomasi J, Cossi M, Millam JM, Klene M, Adamo C, Cammi R, Ochterski JW, Martin RL, Morokuma K, Farkas O, Foresman JB and Fox DJ (2016). Gaussian 16 Rev. C.01. Wallingford, CT.

Hafeez J, Sabir A, Rasool N, Hafeez U, Siddique F, Bilal M, Kanwal A, Ahmad G, Alqahtani F and Imran I (2024). Synthesis of N, N-Bis ([1, 1′-Biphenyl]-4-ylmethyl)-4-morpholinoaniline derivatives via SMC reaction: Assessing their anti-seizure potential through electroencephalogram evaluation and molecular docking studies. *Arab. J. Chem.,* **17**(9): 105889.

Hertwig RH and Koch W (1997). On the parameterization of the local correlation functional. What is Becke-3-LYP? *Chem. Phys. Lett.,* **268**(5): 345-351.

Kabir E. Uzzaman M (2022). A review on biological and medicinal impact of heterocyclic compounds. *Results in Chem.*, **4**: 100606.

Khan IA, Ahmad M, Ashfaq UA, Sultan S and Zaki MEA (2021). Discovery of amide-functionalized benzimidazolium salts as potent α-glucosidase inhibitors. *Molecules* **26**(16): 4760.

Kwiecień H and Wodnicka A (2020). Five-membered ring systems: Furans and benzofurans. *PHC.*, **31**: 281-323.

Little JW, Falace DA, Miller CS and Rhodus NL (2013). Chapter 14 - diabetes mellitus. In: Editors. Little and Falace's Dental Management of the Medically Compromised Patient (Eighth Edition). St. Louis, Mosby. pp.219-239.

Mahat RK, Singh N, Arora M and Rathore V (2019). Health risks and interventions in prediabetes: A review. *DMS: CRR.,* **13**(4): 2803-2811.

Miao YH, Hu YH, Yang J, Liu T, Sun J and Wang XJ (2019). Natural source, bioactivity and synthesis of benzofuran derivatives. *RSC Adv.,* **9**(47): 27510-27540.

Mundhe P, Bhanwala N, Saini SM, Sumanth G, Shivaprasad K, Shende SU, Reddy K and Chandrashekharappa S (2023). Domino synthesis of novel 3-alkenyl benzofuran derivatives- base mediated condensation cascade reaction. *Tetrahedron*, **132**: 133265.

Nair D, Basu P, Pati S, Baseshankar K, Sankara CS and Namboothiri INN (2023). Synthesis of spirolactones and functionalized benzofurans via addition of 3-sulfonylphthalides to 2-formylaryl triflates and conversion to benzofuroisocoumarins. *J. Org. Chem.*, **88**(7): 4519-4527.

Noreen M, Bilal M, Usman Qamar M, Rasool N, Mahmood A, Umar Din S, Ali Shah T, Bin Jardan YA, Bourhia M and Ouahmane L (2024). Facile synthesis of 5-bromo-n-alkylthiophene-2-sulfonamides and its activities against clinically isolated new delhi metallo-β-lactamase producing *Klebsiella pneumoniae* ST147. *Infect Drug Resist.*, pp.2943-2955.

Promchai T, Janhom P, Maneerat W, Rattanajak R, Kamchonwongpaisan S, Pyne SG and Limtharakul T (2020). Antibacterial and cytotoxic activities of phenolic constituents from the stem extracts of Spatholobus parviflorus. *Nat. Prod. Res.,* **34**(10): 1394-1398.

Quasdorf KW, Antoft-Finch A, Liu P, Silberstein AL, Komaromi A, Blackburn T, Ramgren SD, Houk K, Snieckus V and Garg NK (2011). Suzuki- Miyaura cross-coupling of aryl carbamates and sulfamates: Experimental and computational studies. *J. Am. Chem. Soc.*, **133**(16): 6352-6363.

Raghavachari K (2000). Perspective on "Density functional thermochemistry. III. The role of exact exchange". *Theor. Chem. Acc.*, **103**(3): 361-363.

Rauf A, Ahmed F, Qureshi AM, Aziz-ur-Rehman, Khan A, Qadir MI, Choudhary MI, Chohan ZH, Youssoufi MH and Ben Haddad T (2011). Synthesis and urease inhibition studies of barbituric and thiobarbituric acid derived sulphonamides. *J. Chin. Chem. Soc.,* **58**(4): 528-537.

Rubab K, Abbasi MA, Rehman A, Siddiqui SZ, Shah SAA, Ashraf M, Ain Q, Ahmad I, Lodhi MA, Ghufran M, Shahid M and Fatima H (2017). Synthesis, pharmacological screening and computational analysis of some 2-(1H-Indol-3-yl)-N'-[(un)substituted phenylmethylidene] acetohydrazides and 2-(1H-Indol-3-yl)-N'-[(un)substituted benzoyl/2-thienylcarbonyl] acetohydrazides. *Pak. J. Pharm. Sci.,* **30**(4): 1263-1274.

Shahzadi T, Zaib M, Riaz T, Shehzadi S, Abbasi MA and Shahid M (2019). Synthesis of eco-friendly cobalt nanoparticles using celosia argentea plant extract and their efficacy studies as antioxidant, antibacterial,

hemolytic and catalytical agent. *Arab. J. Sci. Eng.*, **44**: 6435-6444.

Sharma U, Naveen T, Maji A, Manna S and Maiti D (2013). Palladium-catalyzed synthesis of benzofurans and coumarins from phenols and olefins. *Angew. Chem., Int. Ed.,* **52**(48): 12669-12673.

Sonia H, Chelleng N, Afzal NU, Manna P, Puzari M, Chetia P and Tamuly C Anti-diabetic and anti-urease inhibition potential of *Amomum dealbatum* Roxb. seeds through a bioassay-guided approach. *Nat. Prod. Res.,* pp.1-6.

Spasov AA, Babkov DA, Prokhorova TY, Sturova EA, Muleeva DR, Demidov MR, Osipov DV, Osyanin VA and Klimochkin YN (2017). Synthesis and biological evaluation of 2-acylbenzofuranes as novel α-glucosidase inhibitors with hypoglycemic activity. *Chem. Biol. Drug Des.,* **90**(6): 1184-1189.

Taha M, Ismail S, Imran S, Almandil NB, Alomari M, Rahim F, Uddin N, Hayat S, Zaman K, Ibrahim M, Alghanem B, Islam I, Farooq RK, Boudjelal M and Khan KM (2022). Synthesis of new urease enzyme inhibitors as antiulcer drug and computational study. *J. Biomol. Struct. Dyn.,* **40**(18): 8232-8247.

Taha M, Rahim F, Ullah H, Wadood A, Farooq RK, Shah SAA, Nawaz M and Zakaria ZA (2020). Synthesis, in vitro urease inhibitory potential and molecular docking study of benzofuran-based-thiazoldinone analogues. *Sci. Rep.,* **10**(1): 10673.

Tollefson EJ, Hanna LE and Jarvo ER (2015). Stereospecific nickel-catalyzed cross-coupling reactions of benzylic ethers and esters. *Acc. Chem. Res.,* **48**(8): 2344-2353.

Ullah H, Khan F and Rahim F (2024). Synthesis, *in vitro* urease inhibitory potential and molecular docking study of thiazolidine-4-one derivatives. *Chem. Data Collect.,* **49**: 101103.

Weatherburn MW (1967). Phenol-hypochlorite reaction for determination of ammonia. *Anal. Chem.,* **39**(8): 971-974.

Xu Xl, Yang Yr, Mo Xf, Wei Jl, Zhang Xj and You Qd (2017). Design, synthesis and evaluation of benzofuran derivatives as novel anti-pancreatic carcinoma agents via interfering the hypoxia environment by targeting HIF-1α pathway. *Eur. J. Med. Chem.,* **137**: 45-62.

Zhou X, Zhang C, Wu J and Zhang G (2013). Association between Helicobacter pylori infection and diabetes mellitus: A meta-analysis of observational studies. *Diabetes Res Clin Pract.,* **99**(2): 200-208.